

Study of Repairing a Corroded Cryogenic Tank by Composite Wrap Subjected to Thermal and Mechanical Loadings

Leila BELKADDOUR*, Mohamed BERRAHOU

University of Ahmed Zabana, GIDD Industrial Engineering and Sustainable Development Laboratory, Relizane, Algeria

Received 11 Jul 2022

Accepted 5 Sep 2022

Abstract

Cryogenic tanks are still considered the most efficient method of storing fluids. This is due to its resistance to much damage caused by corrosion induced by low temperature and internal pressure. In this study, the finite element method is used to analyze the repair performance by a composite wrap in a corroded tank. A parametric analysis was carried out in order to highlight the effects of low temperature and pressure on the thermo-mechanical behavior of the corroded structure and to predict the evolution of stresses in the vicinity of corrosion. An approach to this problem based on the notion of material strength was necessary since it was essential to take both the size of the pre-existing defect and the amount of mechanical stresses. The results obtained show the effect of thermal and mechanical loading to examine their impact on the strength of the structure on the one hand, and on the other hand, the influence of the composite wrap repair in the different corrosion lengths (Path 1, 2, 3) on the reinforcement of the tank. Finally, repairing damage (corrosion) using FRP composites increases the durability of cryogenic tanks, which increases their efficiency their performance and increases their life, although the rate of improvement depends largely on operating conditions, such as pressure and temperature.

© 2022 Jordan Journal of Mechanical and Industrial Engineering. All rights reserved

Keywords: Cryogenic ; tanks; Temperature; Internal Pressure; Corrosion; Finite Element Method (FEM); thermo-mechanical behavior; Von Mises Stress; Fiber Orientation, Composite; wrap..

Nomenclature

R_{ext}	internal radius [mm]
R_{int}	internal radius [mm]
t	thickness of tank [mm]
L	tank length [mm]
A	corrosion depth [mm]
C	half-corrosion length [mm]
t_p	Composite wrap thickness [mm]
L_p	Composite wrap length [mm]
t_a	thickness of adhesive [mm]
s	stacking sequences [mm]
E_1	Young's Modulus in X direction [GPa]
E_2	Young's Modulus in y direction [GPa]
E_3	Young's Modulus in z direction [GPa]
ν_{12}	Poisson Ratio in X-Y plan
ν_{13}	Poisson Ratio in X-Z plan
ν_{23}	Poisson Ratio in Y-Z plan
G_{12}	Shear Modulus in X-Y plan [GPa]
G_{13}	Shear Modulus in X-Z plan [GPa]
G_{23}	Shear Modulus in Y-Z plan [GPa]
CTE	coefficient of thermal expansion [°C]
P_i	internal pressure [MPa]
T_{int}	internal temperature [°C]
T_{ext}	external temperature [°C]

1. Introduction

Storage tanks have long been used in the industrial sector as the most cost-effective and safest method for storing and transporting gas. However, the incidence of accidents has increased significantly as the number of people using them has increased [1-3]. Reinforcement of composite wrap on damaged surfaces is a common local repair approach in the industry [4], to reduce stresses at the corrosion tips and improve the life of the damaged structure [5].

On the basis of bibliographic research, Xugang Wang et al studied the fracture characterization of a 6061 aluminum alloy tube to analyze the mechanism of improvement of the cryogenic forming limit. However, their study was limited to numerical analysis [6]. A study of the effects of surface corrosion damage on the fatigue behavior of 6061 aluminum alloy extrusions was analyzed by Matthew Weber et al [7]. In addition, a numerical study to analyze the transient temperature field and the residual stress distribution caused by the thermal effect in a 6061 aluminum alloy sheet was evaluated by Jianing Wang et al [8]. Sohail et al investigated the behavior of a damaged aluminum aircraft structure repaired with a composite plate under traction using experimental tests and numerical modeling. A parametric study was also conducted for such a repaired cracked plate in order to observe the effect of

* Corresponding author e-mail: lailabelkadour@gmail.com.

the orientation of the fibers and the influence of stress intensity factor lengthening the life of the structure [9, 11]. M. Salem and Faycal Benyahia used numerical modeling to study the behavior of a cracked aluminum plate. The stress intensity factor was calculated for a plate with a horizontal crack under thermo-mechanical loading. The cracked plate was eventually repaired using a composite material, and the effect of this material on fatigue life stress was observed using the finite element method [12]. Mohamed Berrahou et al developed an extensive finite element method to study the thermo-mechanical behavior of a corroded aluminum plate that is repaired with a composite wrap. The effects of patch repair use with different corrosion lengths on stress intensity factor reduction and distribution of damaged areas are also investigated [13, 14]. A number of researchers have evaluated the effectiveness of repair of a tube corroded with a composite material. The uniformity of stress transfer across the enclosed area is the main benefit of the composite repair process, which increases the fatigue life of the repaired structure [15, 17]. Jin-Ho Hong et al conducted a numerical analysis to study corrosion repair from a damaged hydrogen storage tank, determining the effect of variation in winding angle on thermal and mechanical properties [18]. hashin, Zhengyun Hu et al studied the effect of patch type on stress reduction using numerical analysis. They also sought to obtain the best patch shape in a carbon fiber composite polymer when it was glued to a damaged hydrogen storage tank at the center. It has been found that this type of patch is more effective in reducing stress concentration [19]. In his study on a corroded cylindrical tank S.H. Dehghan Manshadi and Mahmoud R. Maheri observed the behavior of fatigue corrosion of a tank through experimental experiments. The storage tank was finally repaired using a composite glass/epoxy polymer patch as a repair procedure using the finite element method [20]. Furthermore, Xiaohang Zhao et al studied the mechanical and thermal behavior of a hydrogen storage tank to determine the influence of the stress distribution and displacement of the stacking sequence [21]. D. Ouinas et al performed a three-dimensional finite element analysis to compare the performance of a carbon/epoxy patch and boron/epoxy patch on a cracked aircraft structure. They demonstrated that the mechanics of the two repair methods are completely different and concluded that the boron/epoxy patch is more efficient [22]. Benyahia et al analyzed the effect of patch shape on stress intensity factor reduction by three-dimensional finite element analysis. The patch shapes considered were rectangular, trapezoidal, circular and elliptical. It was observed that the elliptical shape is more optimal and effective in reducing SIF[23]. Several researchers have performed three-dimensional numerical finite element analysis to determine the best composite patch shape for structural repair [24, 26]. M.Berrahou et al studied the mechanical behavior of a structure damaged by a crack and repaired by different types and forms of patches in order to analyze the effectiveness of the repair. The boron/epoxy patch is the best type used for successful repair by experimental tests and extended finite element method [27]. While doing the library search, we found many researchers who studied domestic hot water tanks, and among these researchers are N. Beithou and M. Abu

Hilal [28-30], who research in this field for multiple goals, such as studying the experimental energy of hot water tanks and thermal analysis of discrete water supply in domestic hot water storage tank. In addition to Ammar Alkhalidi et al., who studied Improving Mixing in Water Aeration Tanks Using Innovative Self-Powered Mixer and Power Reclamation from Aeration Tank [31].

The purpose of this article is a method for strengthening a hydrogen tank with a composite wrap to reduce structural damage in the corroded part. The effect of corrosion length on the variance of Von Mises stresses, in addition to the effect of temperature and pressure on the distribution Von Mises Stress, and finally the effect of fiber orientations on the presence of oval corrosion in a thermo-mechanical loading tank were all examined. This paper is based on modeling and simulation methods to address the risks and failures of a hydrogen storage tank.

2. Geometrical and FE models

2.1. Description of the model

The geometry of the corroded structure considered in this study is shown in Figure 1. Consider the following dimensions for a 6061-T6 aluminum tank see Figure 2: the external radius $R_{ext} = 376$ mm, the internal radius $R_{int} = 364$ mm, the thickness of the tank is $t = 12$ mm, tank length is $L = 1800$ mm.

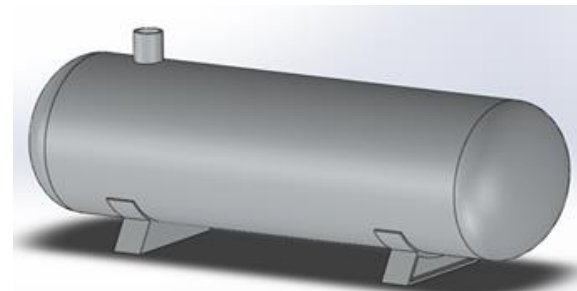


Figure 1. hydrogen tank

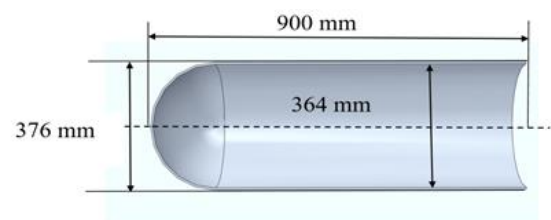


Figure 2. Dimensions of the structure

The longitudinal plan of the tank is used to model corrosion of an ellipsoidal shape. These are defined by their depth -corrosion depth- (a), and their length -half-corrosion length- (c). In this repair, Composite wrap fiber reinforced polymers FRPC has a length L_p of 200mm and a thickness t_{pof} of 6mm. The collage is assured by a thickness of adhesive $t_a=0.2$, in the Figure 3.

For this study, the corroded tank repaired by composite wrap whose ply orientation is of the form $[\mp 45/90/0]$, the plies in the wrap have unidirectional stacking where the fibers are oriented along the length direction, parallel to the load direction as shown in the following table 1

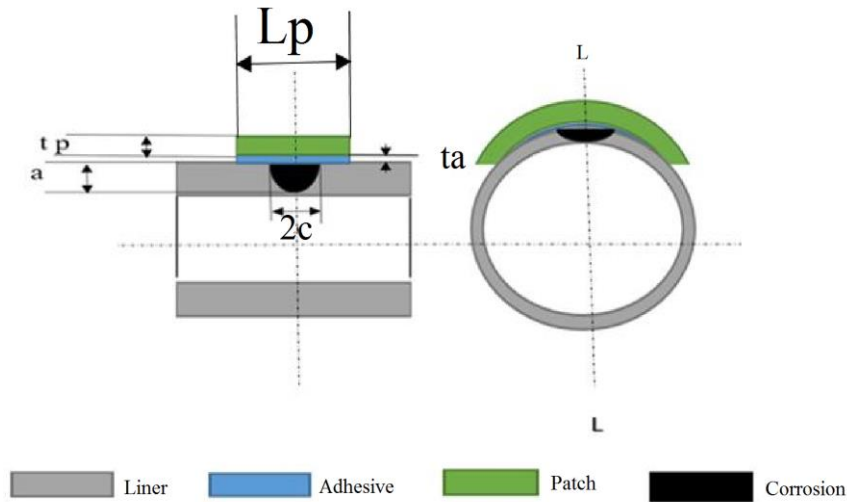


Figure 3. composite wrap repair of ellipsoidal corrosion in a tank

Table 1. Different stacking sequences employed for the composite

	S1	S2	S3	S4	S5
Laminatesequences	[0] _s	[90] _s	[0/45] _s	[0/90] _s	[±45/90/0] _s

The physical properties of the model (wrap, adhesive and liner) are shown in Table 2.

Table 2. Material properties of the tank repair [32-34]

	Type	E ₁ [GPa]	E ₂ [GPa]	E ₃ [GPa]	v ₁₂	v ₁₃	v ₂₃	G ₁₂ [GPa]	G ₂₃ [GPa]	G ₁₃ [GPa]
Liner	Al 6061-T6	68			0.33					
Composite	FRPC	13,94	62.25	94.5	0.2	0.2	0.33	5.415	10.71	4.286
Adhesive	FM73	2,55			0,3					

The thermal properties of the materials are shown in Table 3

Table 3. Thermal properties of the tank materials [33]

	Density (kg.m ⁻³)	CTE (°C ⁻¹)	Thermal conductivity (w.m ⁻¹ .°C ⁻¹)
Liner	2700	2.3×10 ⁻⁵	150
Composite	1560	3.5×10 ⁻⁵	0.2

Table4. The elastic properties of tanks as a function of temperature

Temperature(°C)	-200	-100	25	100	150	200
Young's modulus (MPa)	76500	72700	68900	65800	62700	57700

3. Numerical modeling

The analysis involves a three-dimensional finite element method using the ABAQUS finite element code [35]. Due to the symmetry of the geometry and the applied loads, only a 1/4 model was used. As illustrated in Figure 4, first of all, to analyze the mechanical behavior of the tank at internal pressure and temperature, solid elements with higher order version of the hexahedral linear displacement type were used coupled to temperature C3D8RT, while the element used in the mesh of the corroded part of the cylinder is the tetrahedral linear type C3D4RT. Because this element tolerates irregular shapes without loss of precision, plus the total number of elements generated for this structure is 300888, see Figure 4, the type of element used in the wrap and adhesive is quadratic tetrahedral C3D10. So we kept the same type of element to maintain the precision of the numerical calculation between the thicknesses of the structure. The generation of the wrap band mesh is shown in Figure 5.

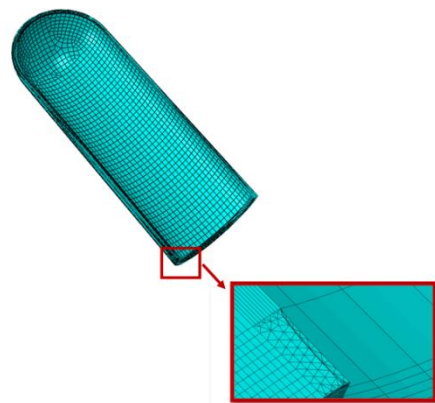


Figure 4. Mesh of the structure and in the vicinity of the corrosion zone

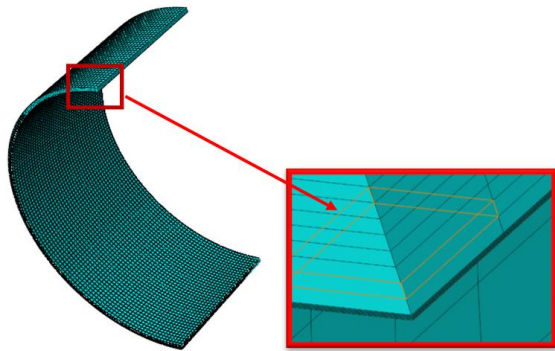


Figure 5. Mesh of the wrap and adhesive

4. Boundary conditions

As a result of the geometric symmetry of the tank, loading internal pressure and temperature and boundary conditions; the model could be reduced to one quarter (1/4) of the structure of symmetry, the longitudinal half and the transverse half.

The reflective symmetry conditions are applied in the longitudinal direction ($U_x = \theta_y = \theta_z = 0$) and in the transverse direction ($U_y = \theta_x = \theta_z = 0$) of one quarter of the structure, see Figure 6.

Figure 7 shows the internal surface of the tank is subjected to mechanical loading of the transported gases under a variant internal pressure $P_i = 35, 30, 25$ and 20 MPa.

The existence of a thermal gradient due to the difference in temperature of the internal surface in contact with the stored gases T_{int} varying between 0 and -250°C and the external surface exposed to the ambient environment $T_{ext} = 20^\circ\text{C}$, In Figure 8.

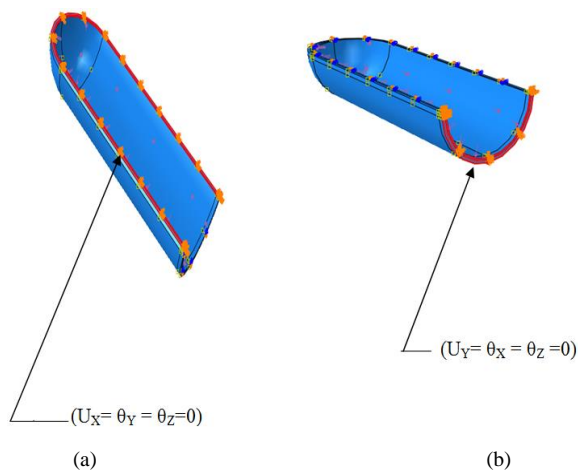


Figure 6. Reflective symmetry conditions, (a) longitudinal direction, (b) transverse direction

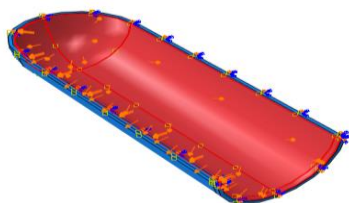
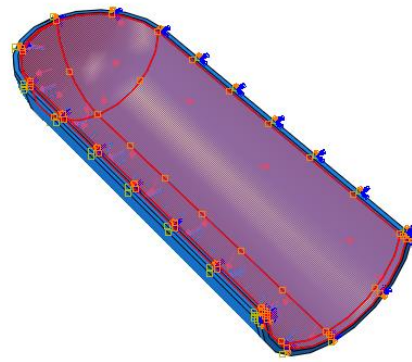
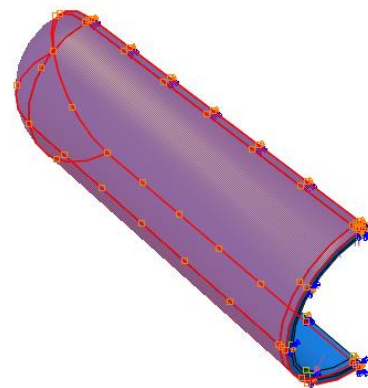


Figure 7. The tank under the internal pressure



(a)



(b)

Figure 8. The tank under thermal loading, (a) internal temperature, (b) external temperature

5. Results and discussion

In this paper, the quality and durability of carbon/epoxy patches with different fiber orientations are examined as shown in Figure 9. The objective of this numerical study is to show the evolution of the Von Mises stress distribution as a function of corrosion length for the three paths and the variation of the maximum Von Mises stresses compared with pressure and temperature.

Yu-Qi Qin et al [33] analyze the failure of the aluminum alloy lining of the vehicle's hydrogen storage tank, which causes cracking during oil circulation, and conduct experimental tests to discover the causes of failure. Maxime Bertin et al [36] evaluated the influence of temperature on the multi layer polymer/composite fatigue behavior and showed the different stresses applied to a hydrogen tank through experimental experiments.

The novelty in our work is the composite patch repair of a corroded cryogenic tank under thermo-mechanical loading to see the effect of temperature and pressure on the distribution of Von stresses and the influence of fiber orientations. All the papers that talk about cryogenic tanks have studied fatigue or structural cracking, but in our research the corrosion behavior has been studied.

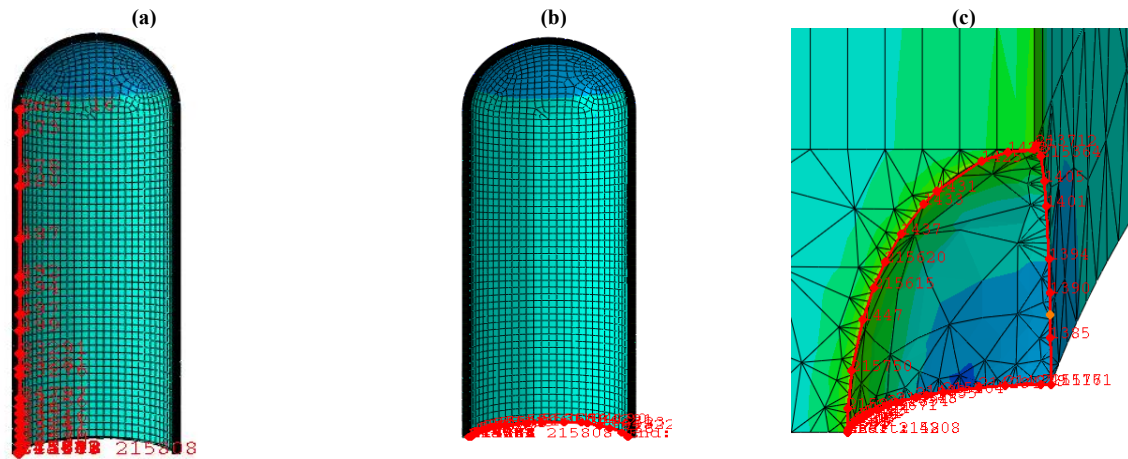


Figure 9. Corrosion length for different directions: (1) path3, (2) path2 and (3) path3

5.1. Effect of corrosion length on the variation of Von Mises stresses for different pressures

Figure 10 shows the variation of Von Mises stress as a function of the longitudinal length (path1) of corrosion for different internal pressures. The presence of pressures, as seen in this figure, minimizes the VonMises stresses exerted on the corrosion point. It can be stated that the increase in longitudinal length generates a considerable decrease in Von Mises stresses. Indeed, an increase in the longitudinal length of the corrosion in the interval [0-13] mm leads to an 80% reduction of the Von Mises stress. This impact is less pronounced for lengths between 13 mm and 55 mm. The values of the Von Mises stress recorded along the tip of the corrosion, for the 20 MPa pressure, are the most inferior to those of the other pressures. The highest value for von Mises stress is recorded when the pressure value is high. In the longitudinal plane, it is also interesting to note that the repair technique used reduces the stress values around the damaged area.

Figure 11 illustrates the influence of the transverse length (Path 2) of corrosion on Von Mises stresses. The increase in this length leads to a decrease in Von Mises stress, until a minimum value of 122 MPa is reached, which corresponds to a transverse length value of 13 mm. We observed that the longitudinal length is influenced more than the transverse length, with stresses being higher than the other direction.

Figure 12 represents the evolution of the Von Mises stresses for different transported gas pressures $P_i = 20; 25; 30$ and 35 MPa. The variation of Von Mises stresses throughout circumferential corrosion reveals that the highest stresses are located in the two corrosion peaks $\theta = 0^\circ$ and 180° . Then, according to this figure, it can be seen that the Von Mises stresses away from the corrosion are stable, while the stresses between the two corrosion peaks are significantly reduced.

Therefore, it can be concluded that the length of the corrosion is strongly affected by the pressure and much more by the temperature at the damaged area.

5.2. Effect of corrosion length on the variation of Von Mises stresses for different temperatures

Figure 13 illustrates the evolution of the Von Mises stress for different temperatures. It shows that the maximum value is recorded at the bottom of the corrosion. It can be seen from this figure that the Von Mises stresses decrease as the longitudinal length (path1) of the corrosion increases. The same behavior was observed for all lengths. Moreover, this variation in stress decreases by increasing the length of the damaged surface. Indeed, the stress evolution for a temperature of 23 k is significantly more important than for a temperature of 173 k, since the temperature of the corroded zone affects the stress distribution.

The temperature effect is shown in Figure 14. The same phenomenon is observed for the variation of VonMises stresses at different temperatures in the longitudinal corrosion direction. VonMises stresses are more highly concentrated at the bottom of the corroded zone, and these stresses decrease as the transverse length (Path 2) of the corrosion tip increases. In addition, the stresses reach minimum values for different temperatures. Beyond this threshold, the distribution tends to produce more or less constant stress levels. It should also be noted that a reduction in temperature reduces the resistance of the liner to mechanical stress, which implies a high risk of structural failure. Longitudinal length is more affected than transverse length because the stresses are greater in one direction than the other.

Figure 15 shows the effect of temperature on the repair of Von Mises stresses as a function of the circumferential length (Path3) of the repaired corrosion. It is noted that the distribution of the opening stress in the vicinity of the corrosion point always has a maximum, after which it gradually slows down to a stable value.

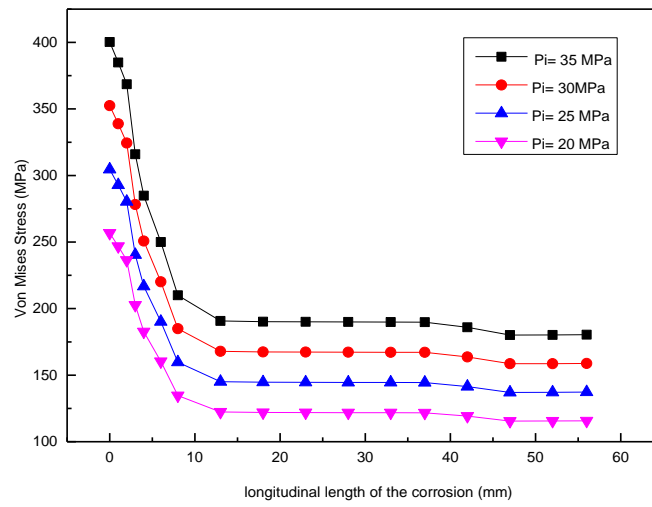


Figure 10. Variation of Von Mises stresses compared to longitudinal corrosion length for different pressures in the case ($a/t=0.5$, $a/c=0.7$)

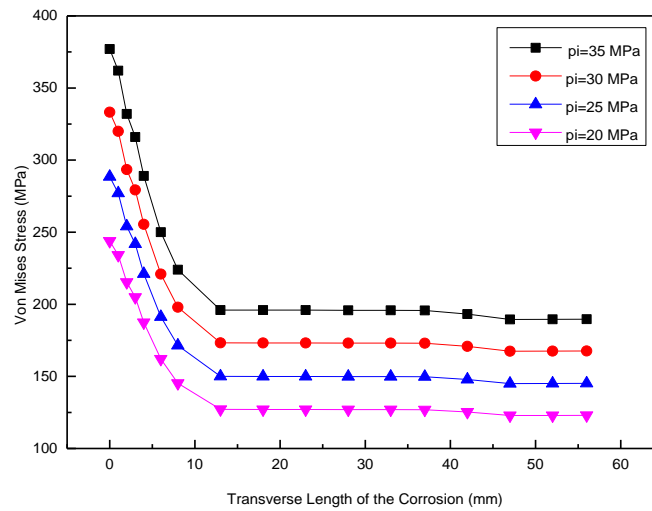


Figure 11. Variation of VonMises stresses compared to the transverse length of the corrosion for different pressures in the case ($a/t=0.5$, $a/c=0.7$)

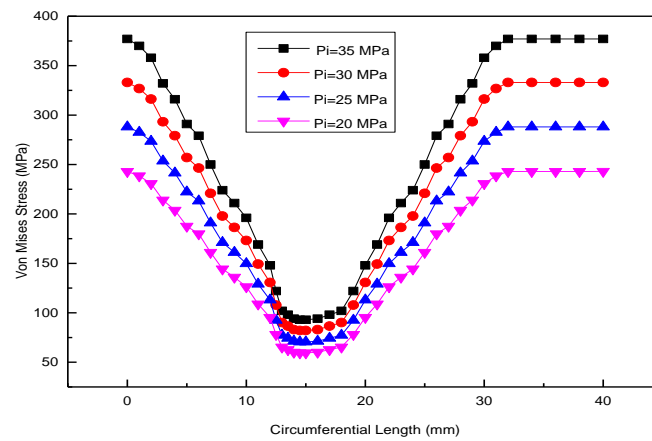


Figure 12. Effect of pressure on Von Mises stress distribution as a function of circumferential length of corrosion in the case ($a/t=0.5$; $a/c=0.5$)

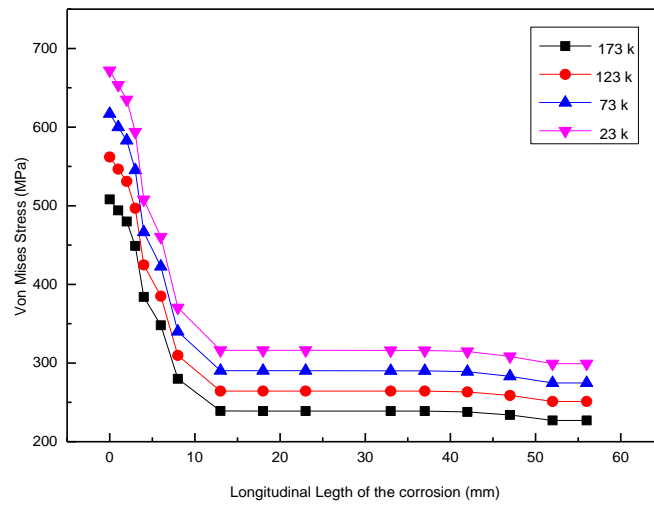


Figure 13. Variation of Von Mises stresses compared to longitudinal length of the corrosion for different temperatures in the case ($a/t=0.5, a/c=0.7$)

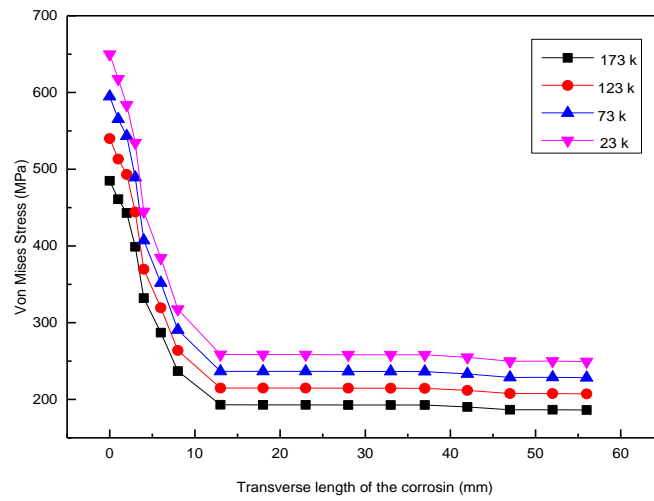


Figure 14. Variation of VonMises stresses compared to transverse length of the corrosion for different temperatures in the case ($a/t=0.5, a/c=0.7$)

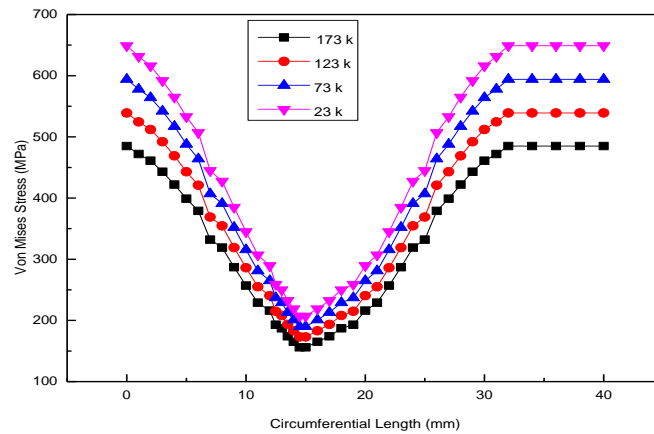


Figure 15. Effect of temperature on the Von Mises stress distribution as a function of the circumferential length of the corrosion in the case ($a/t=0.5; a/c=0.5$).

5.3. Variation of the Von stress as a function of pressure and temperature for the three Paths

The graphs in Figure 16 represent the evolution of the maximum Von Mises stresses as a function of the pressure for the different Paths. Von Mises stresses increases with the increase in internal pressure. The Path 3 shows high values of Von Mises stresses compared to other Paths. The

increase in internal pressure causes a decrease in the concentration of Von Mises stress.

Figure 17 shows the variation of stress as a function of temperature in the various paths. We note that the constraint decreases much more in path2 compared to the other two Path. Also, it can be seen that when the temperature increases, the stress decreases. Thus, the effect of repair is reduced in the transverse direction in relation to the longitudinal and circumferential direction.

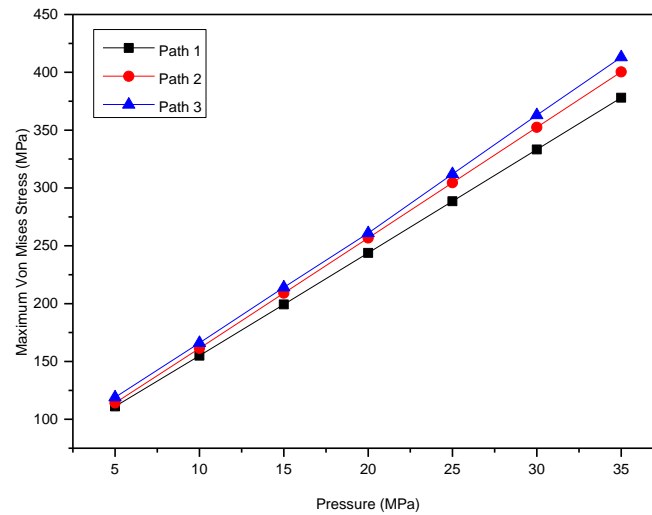


Figure 16. The evolution of the maximum Von Mises stresses as a function of pressure in the case ($a/t=0.5$; $a/c=0.5$).

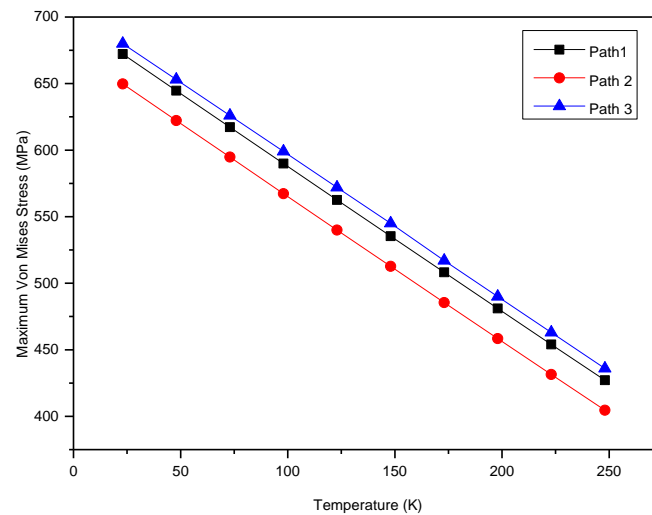


Figure 17. The evolution of the maximum Von Mises stresses as a function of temperature in the case ($a/t=0.5$; $a/c=0.5$)

5.4. The effect of fiber orientation on Von Mises stress repair as a function of corrosion length

Figure 18 shows the effect of the orientation of the fibers on the repair of the VonMises stresses as a function of the longitudinal length of the corrosion. It can be seen that the distribution of Von Mises stresses at the bottom of the defect always has a maximum. This figure also shows that the Von stress decreases when the length increases in the longitudinal direction, beyond the point of corrosion, the variation of the stress will remain constant. It is constant that the carbon/epoxy composite gives a higher value of stress 633 MPa which orients to 0° and 90°, while the values decrease from 600 MPa to 567 MPa for the orientation of the plies is of the form [0/90]s and [0/45]s. Thus, the stacking sequence with the lowest Von Mises stress value is [45/90/0]s.

Figure 19 shows the effect of the orientation of the fibers on the repair of VonMises stresses as a function of the transverse length of the corrosion. In this figure, we observe that the Von Mises stress decreases by oscillation according to the transverse length, beyond the point of corrosion the variation of the stress will remain constant. This same behavior was observed for all the different orientations. As this figure shows, the increase in the Congruence of Von Mises is up to the point of 571MPa upon leaving the wrap of orientation 0° and 90°. While the stresses increase from 540MPa to 507MPa for the orientation of the fibers is of the form [0,45]s and [0,90]s. Among the results obtained, the stacking sequence [45/90/0] is the best since it gives the lowest value of the stresses.

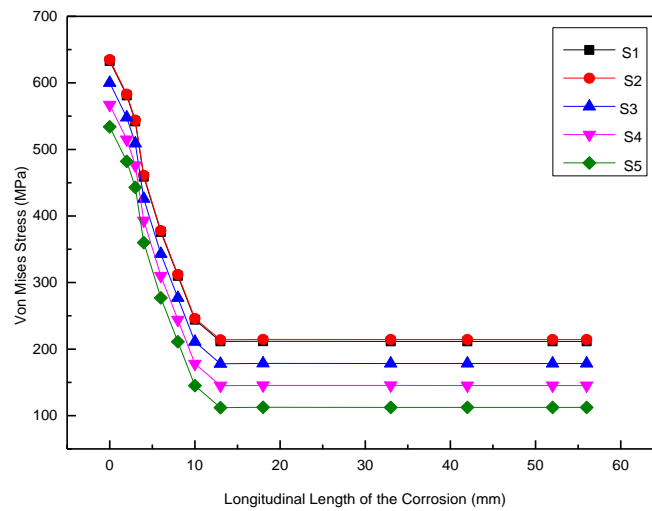


Figure 18. Variation of VonMises stresses compared to longitudinal length of the corrosion for different orientations in the case (a/t=0.5,a/c=0.7)

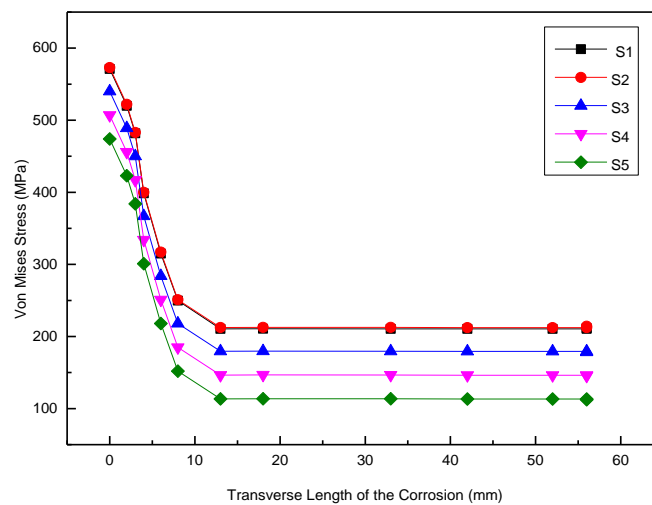


Figure 19. Variation of Von Mises stresses compared to transverse length of the corrosion for different pressure orientations in the case (a/t=0.5,a/c=0.7)

6. Conclusion

This research was part of a broader effort to better understand the corrosion behavior of 6061 aluminum alloy tanks. The results are obtained using the finite element method of a corroded tank repaired by a composite material. The effects of mechanical and thermal loading on the structural strength along with the impact of the length of the corrosion in the three directions, in addition to the influence of the composite wrap repair on the reinforcement of the reservoir, and the effect of the orientation of the fibers on the distribution of the Von stresses all led to the following conclusions:

- As the pressure increases, the Von Mises stress distribution at the bottom of the corrosion also increases.
- The lowering of the temperature of the fluid inside the structure significantly increases the evolution of Von Mises stresses at the level of the corrosion crater.
- Maximum stresses are reached at the lowest temperature, indicating a significant risk of structural failure.
- By increasing the circumferential length of the corrosion, a maximum increase of opening in the vicinity of the corrosion point can be observed.
- The stress increases considerably in the case of circumferential length (path3) compared to the corrosion length for the other Paths of a tank.
- The stress concentration at the corrosion edge is directly affected by the orientation of the wrap. This impact is amplified at the corrosion point.
- wrap repair using fiber-reinforced polymer composites extends the durability of cryogenic tanks, although the rate of improvement is highly dependent on operating conditions, such as pressure and temperature.

References

- [1] M. Abo-Elkhier, and K. Muhammad, "Failure analysis of an exploded large-capacity liquid storage tank using finite element analysis," *Engineering Failure Analysis*, vol. 110, 104401, 2020, doi.org/10.1016/j.engfailanal.2020.104401.
- [2] H. Kacem, and S. Hariri, "Comportement mécanique en statique et en fatigue des aciers à 9% Nickel dans des conditions cryogéniques," In *CFM 23ème Congrès Français de Mécanique*. AFM, Maison de la Mécanique, 39/41 rue Louis Blanc-92400 Courbevoie, 2017.
- [3] Z. Liu, Y. Yang, Y. Liu, and Y. Li, "Effect of gas injection mass flow rates on the thermal behavior in a cryogenic fuel storage tank," *International Journal of Hydrogen Energy*, vol. 47, no. 32, pp. 14703-14713, 2022, doi.org/10.1016/j.ijhydene.2022.02.205.
- [4] P. Cheng, X. J. Gong, S. Aivazzadeh, and X. Xiao, "Experimental observation of tensile behavior of patch repaired composites," *Polymer testing*, vol. 34, pp. 146-154, 2014, doi.org/10.1016/j.polymertesting.2014.01.007.
- [5] H. I. Beloufa, and D. Ouinas, "Renforcement des fissures tridimensionnelle émanant d'entaille circulaire par patch en composite (S06)," In *CFM 2015-22ème Congrès Français de Mécanique*. AFM, Maison de la Mécanique, 39/41 rue Louis Blanc-92400 Courbevoie, 2015.
- [6] W. Xugang, F. Xiaobo, C. Xianshuo, "Forming limit of 6061 aluminum alloy tube at cryogenic temperatures," *Journal of Materials Processing Technology*, vol. 36, pp. 117649, 2022, doi.org/10.1016/j.jmatprotec.2022.117649.
- [7] Weber, Matthew, P.D. Eason, H. Özdeş, and M. Tiryakioğlu, "The effect of surface corrosion damage on the fatigue life of 6061-T6 aluminum alloy extrusions," *Materials Science and Engineering*: vol. 690, pp. 427-432, 2017, doi.org/10.1016/j.msea.2017.03.026.
- [8] J. Wang, X. Chen, L. Yang, and G. Zhang, "Sequentially combined thermo-mechanical and mechanical simulation of double-pulse MIG welding of 6061-T6 aluminum alloy sheets," *Journal of Manufacturing Processes*, vol. 77, pp. 616-631, 2022, DOI:10.1016/j.jmapro.2022.03.046.
- [9] S. M. K. Mohammed, R. Mhamdia, A. Albedah, B. B. Bouiadjra, and F. Benyahia, "Fatigue crack growth in aluminum panels repaired with different shapes of single-sided composite patches," *International Journal of Adhesion and Adhesives*, vol. 105, 102781, 2021, doi.org/10.1016/j.ijadhadh.2020.102781.
- [10] J. J. Schubbe, S. H. Bolstad, and S. Reyes, "Fatigue crack growth behavior of aerospace and ship-grade aluminum repaired with composite patches in a corrosive environment," *Composite Structures*, vol. 144, pp. 44-56, 2016, doi.org/10.1016/j.compstruct.2016.01.107.
- [11] A. K. Bakare, A. A. Shaikh, and S. S. Kale, "Comparison of SCC behaviour of crack in thin aluminium structure with and without single sided composite patch repair," *Engineering Failure Analysis*, vol. 118, 104781, 2020, DOI:10.1016/j.engfailanal.2020.104781.
- [12] M. Salem, M. Berrahou, B. Mechab, and B. B. Bouiadjra, "Analysis of the Adhesive Damage for Different Patch Shapes in Bonded Composite Repair of Corroded Aluminum Plate Under Thermo-Mechanical Loading," *Journal of Failure Analysis and Prevention*, vol. 21, no. 4, pp. 1274-1282, 2021.
- [13] Berrahou, M., Mokadem, S., Mechab, B., & Bachir Bouiadjra, B. "Effect of the corrosion of plate with double cracks in bonded composite repair," *Struct. Eng. Mech*, vol. 64, no. 3, pp. 323-328, 2017, doi.org/10.1590/1516-1439.259613.
- [14] A. K. Bakare, A. A. Shaikh, and S. S. Kale. "Corrosion behaviour of stop-hole and notch instead of crack in thin aluminium alloy sheet repaired with bonded patch exposed to saline environment under constant load," *Engineering Failure Analysis*, vol. 120, 105067, 2021, doi.org/10.1016/j.engfailanal.2020.105067.
- [15] M. W. Junior, J. M. L. Reis, and C. Mattos, "Polymer-based composite repair system for severely corroded circumferential welds in steel pipes," *Engineering Failure Analysis*, vol. 81, pp. 135-144, 2017, doi.org/10.1016/j.engfailanal.2017.08.001.
- [16] D. M. Ryu, L. Wang, S. K. Kim, and J. M. Lee, "Comparative study on deformation and mechanical behavior of corroded pipe: Part I-Numerical simulation and experimental investigation under impact load," *International Journal of Naval Architecture and Ocean Engineering*, vol. 9, no. 5, pp. 509-524, 2017, doi.org/10.1016/j.ijnaoe.2017.01.005.
- [17] M. Perl, and T. Saley, "The detrimental effect of autofrettage on externally cracked modern tank gun barrels," *Defence Technology*, vol. 15, no. 2, pp. 146-153, 2019, doi.org/10.1016/j.dt.2018.10.001.
- [18] J. H. Hong, M. G. Han, and S. H. Chang, "Safety evaluation of 70 MPa-capacity type III hydrogen pressure vessel considering material degradation of composites due to temperature rise," *Composite Structures*, vol. 113, pp. 127-133, 2014, doi.org/10.1016/j.compstruct.2014.03.008.
- [19] Z. Hu, M. Chen, and B. Pan, "Simulation and burst validation of 70 MPa type IV hydrogen storage vessel with dome reinforcement," *International Journal of Hydrogen Energy*, vol. 46, no. 46, pp. 23779-23794, 2021, doi.org/10.1016/j.ijhydene.2021.04.186.

- [20] S. D. Manshadi, and M. R. Maheri, "The effects of long-term corrosion on the dynamic characteristics of ground based cylindrical liquid storage tanks," *Thin-Walled Structures*, vol. 48, no. 12, pp. 888-896, 2010, doi.org/10.1016/j.tws.2010.05.003.
- [21] X. Zhao, Y. Yan, J. Zhang, F. Zhang, Z. Wang, and Z. Ni, "Analysis of multilayered carbon fiber winding of cryo-compressed hydrogen storage vessel," *International Journal of Hydrogen Energy*, vol. 47, no. 20, pp. 10934-10946, 2022, doi.org/10.1016/j.ijhydene.2022.01.136.
- [22] D. Ouinas, B. B. Bouiadjra, and B. Serier, "The effects of disbands on the stress intensity factor of aluminium panels repaired using composite materials," *Composite structures*, vol. 78, no. 2, pp. 278-284, 2007, doi.org/10.1016/j.compstruct.2005.10.012.
- [23] F. Benyahia, A. Albedah, and B. B. Bouiadjra, "Elliptical and circular bonded composite repair under mechanical and thermal loading in aircraft structures," *Materials Research*, 17(5), 1219-1225, (2014).
- [24] M. Salem, M. Berrahou, B. Mechab, and B. B. Bouiadjra, "Effect of the angles of the cracks of corroded plate in bonded composite repair," *Frattura ed Integrità Strutturale*, vol. 12, no. 46, pp. 113-123, 2018, doi:10.3221/IGF-ESIS.46.12.
- [25] H. Benzineb, M. Berrahou, and M. Serier, "Analysis of the adhesive damage for different shapes and types patch's in corroded plates with an inclined crack," *Frattura e Integrità Strutturale*, vol. 60, 2022, doi.org/10.3221/IGF-ESIS.60.23 .
- [26] M. Berrahou, and B. B. Bouiadjra, "Analysis of the adhesive damage for different patch shapes in bonded composite repair of corroded aluminum plate," *Structural engineering and mechanics: An international journal*, vol. 59, no.1, pp. 123-132, 2016, DOI:10.12989/sem.2016.59.1.123.
- [27] K. Amari, and M. Berrahou. "Experimental and Numerical Study of the Effect of Patch Shape for Notched Cracked Composite Structure Repaired by Composite Patching," *Journal of Failure Analysis and Prevention*, vol. 22, no. 3, pp.1040-1049, 2022, doi.org/10.1007/s11668-022-01391-z.
- [28] N. Beithou, M. Abu Hilal, " Experimental Energy Study for Domestic Hot Water Storage Tanks," *Jordan Journal of Mechanical and Industrial Engineering*, Vol. 5, no. 5, pp. 471 – 477, 2011.
- [29] N. Beithou, M. Abu Hilal, I. Abu-Alshaiikh, " Thermal Analysis of Discrete Water supply in Domestic Hot Water Storage Tank," *Jordan Journal of Mechanical and Industrial Engineering*, Vol. 5 , no. 1, pp. 29- 32, 2011.
- [30] N. Beithou , M. Abu Hilal, " Hot Water Management of DHW Storage Tank: Supply Features," *Jordan Journal of Mechanical and Industrial Engineering*, Vol. 4, no. 6, pp. 789- 796, 2010.
- [31] Ammar A. T. Alkhalidi, Patrick Bryar, Ryo S. Amano, "Improving Mixing in Water Aeration Tanks Using Innovative Self-Powered Mixer and Power Reclamation from Aeration Tank," *Jordan Journal of Mechanical and Industrial Engineering*, Vol. 10, no. 3, pp. 211-214, 2016.
- [32] H. Qiu, M. Enoki, Y. Kawaguchi, and T. Kishi, "A model for the static fracture toughness of ductile structural steel," *J. Engineering Fracture Mechanics*, vol. 70, pp. 599–609, 2003, doi.org/10.1016/S0013-7944(02)00079-6.
- [33] Y. Q. Qin, Y. Gong, Y. W. Yuan, and Z. G. Yang, "Failure analysis on leakage of hydrogen storage tank for vehicles occurring in oil circulation fatigue test," *Engineering Failure Analysis*, vol. 117, 104830, 2020, doi.org/10.1016/j.engfailanal.2020.104830.
- [34] S. Fintová, I. Kuběna, L. Trško, V. Horník, and L. Kunz, "Fatigue behavior of AW7075 aluminum alloy in ultra-high cycle fatigue region," *Mater. Sci. Eng.*, vol. 774, 138922, 2020, doi.org/10.1016/j.msea.2020.138922.
- [35] ABAQUS Standard/User's Manual, Version 6.11. Hibbit Karlsson & Sorensen, Inc., Pawtucket, RI, USA, 2007.
- [36] M. Bertin, F. Touchard, M.C. Lafarie-Frenot, "Experimental study of the stacking sequence effect on polymer/composite multi-layers submitted to thermomechanical cyclic loadings," *International Journal of Hydrogen Energy*, vol. 35, no. 20, pp.11397-11404, October 2010, doi:10.1016/j.ijhydene.2010.07.018.